

R.J. Marks II, M.I. Jones, E.L. Kral and J.F. Walkup, "One-dimensional linear coherent processing using a single optical element", *Applied Optics*, vol. 18, pp.2783-2786 (1979).

One-dimensional linear coherent processing using a single optical element

Robert J. Marks II, Mike I. Jones, E. Lee Kral, and John F. Walkup

A coherent processor is presented which is capable of performing a large class of 1-D linear space-variant operations. The only components of the processor are a 1-D input, a mask whose transmittance is specified by the desired linear operation, and an output plane. Compared with other 1-D processors, this processor has advantages of real space compactness and total elimination of vignetting. Experimental results are presented for the specific operations of convolution and spectrum scaling.

I. Introduction

A generalized technique for coherent linear space-variant processing was initially discussed by Cutrona.¹ Alternate techniques for performing 1-D space-variant operations have recently been reported.²⁻⁴ Each of these processors requires a 1-D input, a mask (whose transmittance determines the linear operation), and a system of cylindrical and/or spherical lenses. In this paper, we describe such a processor which requires only a single optical element. Real space compactness and vignetting elimination are achieved. An inherent assumption in the design is that the processor's output intensity (rather than phase and amplitude) is of interest. As will be shown, however, the output's phase and amplitude can be preserved by the simple inclusion of a lens immediately prior to the processor output plane.

II. Preliminaries

A linear space-variant operation can be described via the superposition integral:

$$g(x) = \int_{-\infty}^{\infty} u(\xi)h(x;\xi)d\xi. \quad (1)$$

Here, $g(\cdot)$ is the output of a system with line-spread function (impulse response) $h(\cdot, \cdot)$ corresponding to an input $u(\cdot)$.

We will show that the familiar Fourier transform configuration shown in Fig. 1 is capable of performing the general space-variant operation.⁵ A 1-D input $u(\xi)$ is placed in plane $P1$, directly adjacent to a mask with transmittance $H(f_x;\xi)$ given by

$$H(f_x;\xi) = \int_{-\infty}^{\infty} h(x;\xi) \exp(j2\pi f_x x) dx. \quad (2)$$

The spatial frequency variable f_x is measured by dividing the actual vertical spatial displacement in plane $P1$ by $\lambda\ell$, where ℓ is the focal length of the spherical lens, and λ is the wavelength of the coherent plane wave illumination. Note, through Fourier transform inversion, that

$$h(x;\xi) = \int_{-\infty}^{\infty} H(f_x;\xi) \exp(-j2\pi f_x x) df_x. \quad (3)$$

The product $u(\xi)H(f_x;\xi)$ is Fourier transformed by the thin lens in Fig. 1 to give incident on plane $P2$ the field amplitude^{6,7}

$$g_0(x;\nu) = \iint_{-\infty}^{\infty} u(\xi)H(f_x;\xi) \exp[-j2\pi(f_x x + \xi\nu)] df_x d\xi, \quad (4)$$

where ν , the frequency variable associated with ξ , is measured identically to the method described for f_x . From Eq. (3), it follows that

$$g_0(x;\nu) = \int_{-\infty}^{\infty} u(\xi)h(x;\xi) \exp(-j2\pi\nu\xi) d\xi. \quad (5)$$

Comparing with the superposition integral in Eq. (1), we conclude

$$g(x) = g_0(x;0). \quad (6)$$

That is, the desired 1-D output lies along the x axis in plane $P2$ of the processor. The familiar thin lens Fourier transform configuration of Fig. 1 is thus seen to be capable of performing a wide class of linear space-variant operations.

Robert J. Marks II is with University of Washington, Department of Electrical Engineering, Seattle, Washington 98195; the other authors are with Texas Tech University, Department of Electrical Engineering, Lubbock, Texas 79409.

Received 16 October 1978.

0003-6935/79/162783-04\$00.50/0.

© 1979 Optical Society of America.

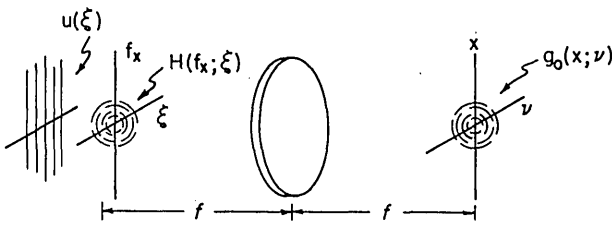


Fig. 1. A coherent processor for performing 1-D space-variant operations. The desired output appears along the x axis in plane $P2$.

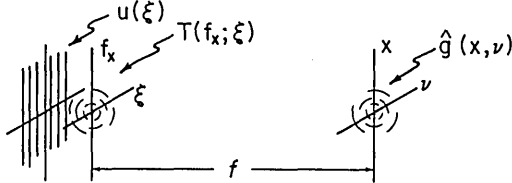


Fig. 2. The generalized single optical element 1-D space-variant processor requires only an input $u(\cdot)$, a mask $T(f_x; \xi)$, and an output plane.

III. Single Optical Element Processor

If we are interested only in the intensity distribution on plane $P2$ of Fig. 1, the input transmittance and mask can be moved directly adjacent the spherical lens.⁸ The lens transmittance can now be included on the mask to give a revised mask transmittance of

$$T(f_x; \xi) = H(f_x; \xi) \exp\left\{\frac{-j\pi}{\lambda f} [\xi^2 + (\lambda f f_x)^2]\right\}. \quad (7)$$

(Recall $x = \lambda f f_x$ is the vertical displacement on plane $P1$.) The resulting processor, pictured in Fig. 2, requires only a 1-D transmittance placed adjacent a mask. It is difficult to imagine a coherent processor in more compact form. Note also that vignetting⁸ is totally eliminated. The actual field amplitude incident on plane $P2$ of this processor can easily be shown to be⁸

$$\hat{g}_0(x; \nu) = g_0(x; \nu) \exp\left\{\frac{j\pi}{\lambda f} [x^2 + (\lambda f \nu)^2]\right\}. \quad (8)$$

The intensity distribution on the output planes of the processors in Figs. 1 and 2 are identical, that is,

$$|\hat{g}_0(x; \nu)|^2 = |g_0(x; \nu)|^2. \quad (9)$$

The desired modulus squared of the space-variant operation result can be viewed along the x axis of the processor's output plane. Note that the phase term in Eq. (8) can be removed simply by placing a convex lens of focal length f immediately prior to the processor output. Since we are interested in only the field amplitude along the x axis, a cylindrical lens would also suffice. In either case, the processor output would yield the desired result both in amplitude and phase. This condition, for example, would be required if further processing were to be performed on the system output.

IV. Examples

We now present two example applications of the single optical element 1-D space-variant processor with experimental results.

A. Convolution (Space Invariant)

The linear operation of convolution is defined as

$$g(x) = \int_{-\infty}^{\infty} u(\xi)h(x - \xi)d\xi. \quad (10)$$

From Eq. (2) it follows that

$$H(f_x; \xi) = \hat{H}(f_x) \exp(j2\pi f_x \xi), \quad (11)$$

where $\hat{H}(f_x)$ is related to $h(x)$ by a Fourier transform:

$$\hat{H}(f_x) = \int_{-\infty}^{\infty} h(x) \exp(j2\pi f_x x) dx. \quad (12)$$

The desired mask transmittance is thus

$$T(f_x; \xi) = \hat{H}(f_x) \exp\left\{\frac{-j\pi}{\lambda f} (\xi - \lambda f f_x)^2\right\}. \quad (13)$$

The exponential term is recognized as the transmittance of a cylindrical lens with focal length $f_c = f/2$ rotated 45° in the (ξ, f_x) -plane. We thus can generate the T mask by placing a 1-D transmittance of $\hat{H}(f_x)$ adjacent to a rotated lens.

An interesting, although trivial, application of the convolution processor is 1-D unit magnification imaging. Since the corresponding $\hat{H}(f_x)$ is identically one for all f_x , this operation can be achieved with only the 45° rotated cylindrical lens.

The experiment chosen to illustrate the convolution processor is the performance of an autoconvolution of a single pulse [Fig. 3(a)]. The result is shown in Fig. 3(b). The squared modulus of the result is pictured in Fig. 3(c). This is the intensity distribution we should observe along the x axis of the processor output.

The line-spread function pictured in Fig. 3(a) can be expressed as

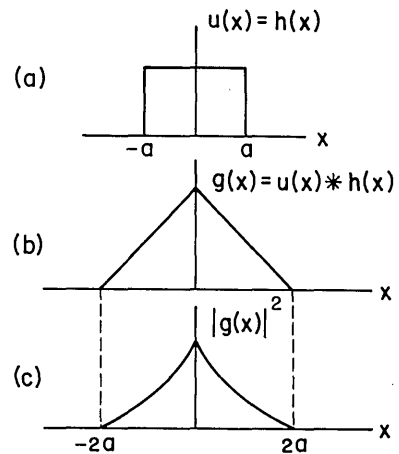


Fig. 3. Convolving the pulse in (a) with itself gives the result in (b). The output of the 1-D convolution processor will give the intensity distribution shown in (c).

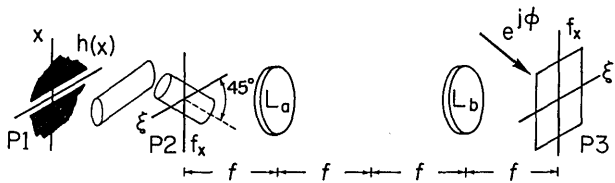


Fig. 4. A scheme for recording the mask required for the convolution processor. The transforming cylindrical lens has twice the focal length of the rotated cylindrical lens.

$$h(x) = \begin{cases} 1; & |x| \leq a \\ 0; & |x| > a \end{cases}, \quad (14)$$

where $2a$ is the pulse width. It follows that the desired mask transmittance is

$$T(f_x; \xi) = 2a \operatorname{sinc}(2af_x) \exp\left[\frac{-j\pi}{\lambda f} (\xi - \lambda f f_x)^2\right], \quad (15)$$

where $\operatorname{sinc}x = (\sin\pi x)/\pi x$.

The mask transmittance is generated as shown in Fig. 4.⁹ This impulse response $h(x)$, pictured in Fig. 3(a), is placed on $P1$ and is Fourier transformed by a single cylindrical lens. Thus, the desired $\hat{H}(f_x)$ is incident on plane $P2$, where it is multiplied by the transmittance of the rotated cylindrical lens. Note that in order for f_x to be measured in the previously discussed manner, we require that the transforming lens have twice the focal length of the rotated lens.

Except for coordinate reversal, the field amplitude which exits plane $P2$ is the desired relationship for $T(f_x; \xi)$. To holographically record this relation, spherical lenses L_a and L_b perform a conventional imaging operation onto plane $P3$, which is also illuminated by a planar reference beam $e^{j\phi}$. The photosensitive medium in plane $P3$, when processed, will then serve as the holographic mask for the processor in Fig. 2.

By using the same pulse in Fig. 3(a) as the processor input, convolution is performed. A picture of the processor output is shown in Fig. 5, and a 1-D scan of the x axis is shown in Fig. 6. As can be seen, the result compares favorably with Fig. 3(c).

B. Spectrum Scaling (Space Variant)

A second example application of the single optical element processor is in the scaling of the Fourier transform or spectrum of a 1-D signal. The input-output relationship here is given by

$$g(x) = \int_{-\infty}^{\infty} u(\xi) \exp\left(\frac{-j2\pi}{M\lambda f} x\xi\right) d\xi, \quad (16)$$

where M is a dimensionless scaling factor. The spectrum of $u(\cdot)$ can be written as

$$U(\nu) = \int_{-\infty}^{\infty} u(\xi) \exp(-j2\pi\nu\xi) d\xi. \quad (17)$$

Comparing with Eq. (16), we conclude that

$$g(x) = U[x/(M\lambda f)]. \quad (18)$$

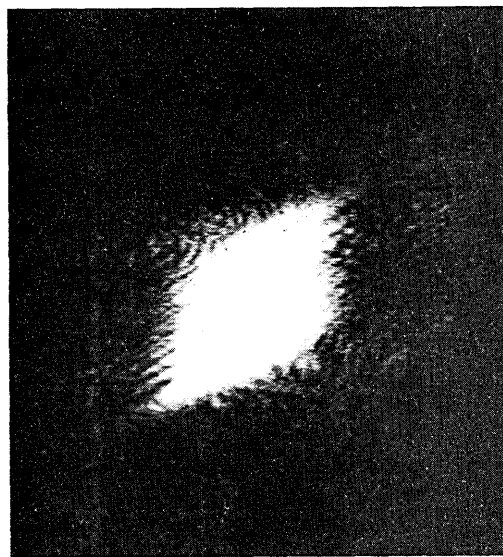


Fig. 5. The output of the convolution processor for a double pulse input. The intensity distribution along the x axis should be the same as Fig. 3(c).

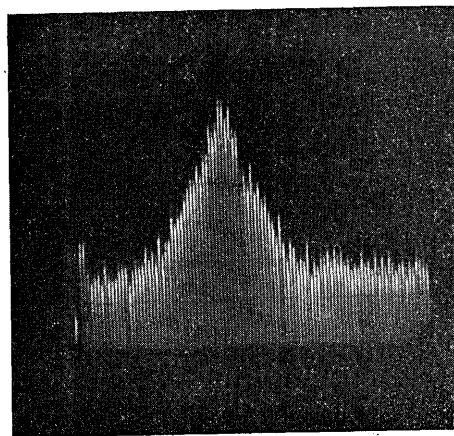


Fig. 6. A scan of the x axis of Fig. 5. The results compare favorably with Fig. 3(c).

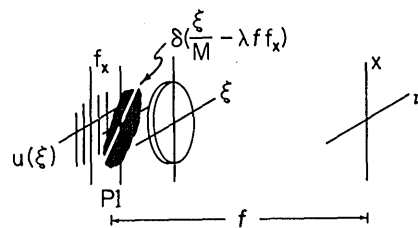


Fig. 7. A processor for performing spectrum scaling. The slope of the slit is equivalent to the spectral magnification.

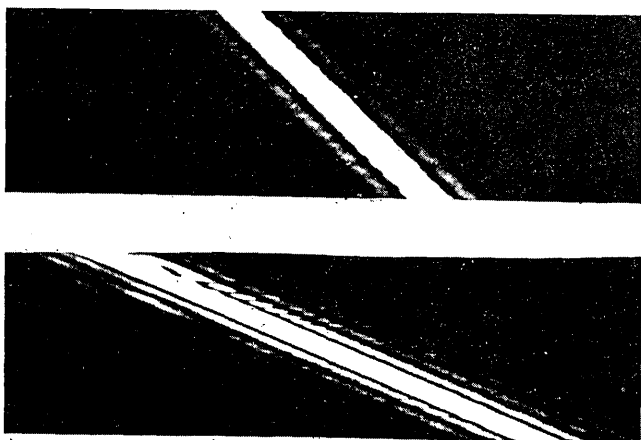


Fig. 8. Outputs of the spectral magnifier in Fig. 7 for a single pulse input corresponding to two magnifications.

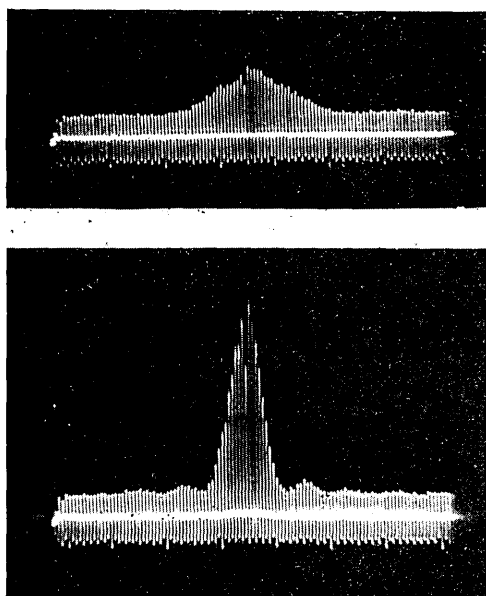


Fig. 9. x -axis scans of Fig. 8.

The scaling operation is now more clearly seen. The parameter M can be interpreted as the spectral magnification.

The impulse response of the spectrum magnifier is

$$h(x;\xi) = \exp[-j2\pi x\xi / (M\lambda f)]. \quad (19)$$

After some computation, it follows that

$$T(f_x;\xi) = \delta\left(\frac{\xi}{M} - \lambda f f_x\right) \exp\left[\frac{-j\pi}{\lambda f} (\xi^2 + \lambda f f_x^2)\right]. \quad (20)$$

The desired mask is thus the product of a Dirac delta and a spherical lens transmittance. The Dirac delta term can be interpreted as an impulse sheet lying along the line $\xi = M\lambda f f_x$ in the (ξ, f_x) -plane. Recalling again that $\lambda f f_x$ is a measure of spatial displacement, we conclude that the slope of this line is the spectral magnification M .

The single optical element coherent processor for performing spectral magnification is shown in Fig. 7. The input $u(\xi)$ is placed in plane $P1$ directly adjacent a thin slit, which corresponds to the Dirac delta term. A spherical lens is also placed on plane $P1$.

Experimental results of the spectrum magnifier output plane are shown in Fig. 8 for the case of a single pulse input for two values of M . The corresponding x -axis scans are shown in Fig. 9.

V. Conclusions

We have presented a coherent processor capable of performing generalized 1-D linear space-variant operations with the use of only a single optical element. The advantages of this over previously presented 1-D space-variant processors include superior real space compactness and total elimination of vignetting. The performance of the processor was illustrated through implementation of the specific operations of convolution and spectral magnification.

This work was generously supported by the University of Washington Graduate School Research Fund (Project PSE-517) and by AFOSR grant 75-2855.

References

1. L. J. Cutrona, "Recent Developments in Coherent Optical Technology," in *Optical and Electro-Optical Information Processing*, J. T. Tippet *et al.*, Eds. (MIT Press, Cambridge, 1965).
2. W. T. Rhodes and J. M. Florence, *Appl. Opt.* **15**, 3073 (1976).
3. J. W. Goodman, P. Kellman, and E. W. Hansen, *Appl. Opt.* **16**, 733 (1977).
4. R. J. Marks II, J. F. Walkup, M. O. Hagler, and T. F. Krile, *Appl. Opt.* **16**, 739 (1977).
5. W. T. Rhodes, Georgia Inst. of Technology; private communication (8 October 1976).
6. F. P. Carlson, *Introduction to Applied Optics for Engineers* (McGraw-Hill, New York, 1976).
7. Here and henceforth, proportionality constants for field amplitudes and transmittances are omitted since they add nothing to the theory development or experiment description.
8. J. W. Goodman, *Introduction to Fourier Optics* (McGraw-Hill, New York, 1968).
9. If $H(f_x;\xi)$ is a more complicated complex or bipolar function, it can be formed via a computer generated hologram. The lens transmittance portion of the T mask, however, contains spatial frequencies which are too high to be formed by conventional low-cost computer-generated holograms. Thus, the H and lens transmittances can either be placed back-to-back or, as in this section, combined into a single holographic transmittance.